Automated coronary artery tree extraction in coronary CT angiography using a multiscale enhancement and dynamic balloon tracking (MSCAR-DBT) method

Chuan Zhou*, Heang-Ping Chan, Aamer Chughtai, Smita Patel, Lubomir M. Hadjiiski, Jun Wei, Ella A. Kazerooni

Department of Radiology, University of Michigan, Ann Arbor, United States

ARTICLE INFO

ABSTRACT

Rational and objectives: To evaluate our prototype method for segmentation and tracking of the coronary arterial tree, which is the foundation for a computer-aided detection (CADe) system to be developed to assist radiologists in detecting non-calcified plaques in coronary CT angiography (cCTA) scans.

Materials and methods: The heart region was first extracted by a morphological operation and an adaptive thresholding method based on expectation-maximization (EM) estimation. The vascular structures within the heart region were enhanced and segmented using a multiscale coronary response (MSCAR) method that combined 3D multiscale filtering, analysis of the eigenvalues of Hessian matrices and EM estimation segmentation. After the segmentation of vascular structures, the coronary arteries were tracked by a 3D dynamic balloon tracking (DBT) method. The DBT method started at two manually identified seed points located at the origins of the left and right coronary arteries (LCA and RCA) for extraction of the arterial trees. The coronary arterial trees of a data set containing 20 ECG-gated contrast-enhanced cCTA scans were extracted by our MSCAR-DBT method and a clinical GE Advantage workstation. Two experienced thoracic radiologists visually examined the coronary arteries on the original cCTA scans and the rendered volume of segmented vessels to count the untracked false-negative (FN) segments and false positives (FPs) for both methods.

Results: For the visible coronary arterial segments in the 20 cases, the radiologists identified that 25 segments were missed by our MSCAR-DBT method, ranging from 0 to 5 FN segments in individual cases, and that 55 artery segments were missed by the GE software, ranging from 0 to 7 FN segments in individual cases. 19 and 15 FPs were identified in our and the GE coronary trees, ranging from 0 to 4 FPs for both methods in individual cases, respectively.

Conclusion: The preliminary study demonstrates the feasibility of our MSCAR-DBT method for segmentation and tracking coronary artery trees. The results indicated that both our method and GE software can extract coronary artery trees reasonably well and the performance of our method is superior to that of GE software in this small data set. Further studies are underway to develop methods for improvement of the segmentation and tracking accuracy.

1. Introduction

Coronary artery disease (CAD) is the most common type of heart disease and the leading cause of death worldwide [1]. CAD is a condition in which atheromatous plaques build up inside the coronary arteries. When the coronary arteries are narrowed or blocked, the reduction of oxygen-rich blood flow to the heart muscle can cause angina or a myocardial infarction (MI). Over 16 million Americans have coronary heart disease (CHD) and the prevalence of MI approaches 8 millions [2]. Over 445,000 Americans die of CHD and over 151,000 die of MI each year. With the rapid advancement of CT technique, ECG-gated contrast-enhanced coronary computed tomography angiography (cCTA) permits visualization of the vessel lumen, atherosclerotic plaque, and stenoses without the invasive catheterization procedure. cCTA is becoming the most promising modality for assessing coronary heart disease and for quantifying the plaques [3–6].

Accurate identification of plaques is challenging, especially for the noncalcified plaques, due to many factors such as the small size of coronary arteries, reconstruction artifacts caused by irregular heart beats, beam hardening, and partial volume averaging. The advent of 16, 32, 64 and the latest 320 row multidetector CT

* Corresponding author at: Department of Radiology, University of Michigan, CGC B2103 1500 E. Medical Center Drive, Ann Arbor, MI 48109, United States.
Tel.: +1 734 647 8554; fax: +1 734 615 5513.
E-mail address: chuan@umich.edu (C. Zhou).

not only increases the spatial and the temporal resolution significantly, but also increases the number of images to be interpreted by radiologists substantially. Radiologists have to visually examine each coronary artery for suspicious stenosis using visualization tools such as multiplanar reformatting (MPR) and curved planar reformatting (CPR) provided by the review workstation in clinical practice. However, these visualization tools depend on the accurate extraction of coronary arteries. Automatic extraction of the coronary artery trees will reduce the time for coronary analysis. The coronary artery extraction software of the commercial systems is still evolving – some require interactive user-input starting and ending points of the artery of interest, and others attempt to automatically extract the coronary arterial trees without user input. The performance of the commercial software varies from vendor to vendor. For a given vendor, the performance still changes from version to version and the trade-off between sensitivity and specificity varies. However, no vendor software can automatically detect and identify the coronary artery segment with non-calcified plaques and perform MPR or CPR on the coronary artery segment of interest to further speed up coronary analysis.

Because plaques only occur in coronary arteries, the extraction of the coronary arteries constitutes the fundamental step in the detection of plaques. Many of the published studies of vessel segmentation and tracking were performed on 2D or 3D images for vascular structures in the retina, liver, brain and lung. Few studies have been conducted for automated segmentation, tracking and construction of the entire coronary artery trees on cCTA images. The methods used in vessel segmentation and tracking included hysteresis thresholding [7], region growing [8,9], statistical modeling and matching methods [10,11] using *a priori* knowledge provided by radiologists, direction field based segmentation and detection [12] and deformable model approaches [13,14] in which an initial surface estimate was deformed iteratively to optimize an energy criterion so that the model boundary was extended to the vessel wall as a so-called minimal surface. Multiscale filtering has been used for the segmentation of curvilinear or tubular structures in 3D medical images [15–22]. The conventional multiscale filtering methods [15,20,23] have been widely used to enhance the vascular structures at variable sizes for vessel extraction, in which the images are convolved with 3D Gaussian filters at multiple scales and the eigenvalues of the Hessian matrix at each voxel are analyzed in terms of a response function to extract local structures in the image. The design of the response function is a critical factor that determines the specific shape to be enhanced and therefore whether the multiscale method is effective for a given application. In a recent study [24], a minimum cost path approach was used to extract coronary artery centerline connecting user-defined starting and ending points in cCTA images. Two different cost functions, multiscale vesselness cost function based on eigenvalues of Hessian matrix of images, and region statistics cost function were evaluated. The results show that 88% and 47% of the vessel centerlines were correctly extracted using the vesselness and region statistics cost function, respectively.

We are developing a computer-aided detection (CADe) system to assist radiologists in detecting non-calcified plaques in cCTA scans and automatically identifying the vessels of interest. Our basic approach to enhancement and segmentation of the coronary arterial trees is similar to the vascular structure enhancement and segmentation methods that we designed for the pulmonary vessels in CT pulmonary angiographic (CTPA) scans [25]. However, since the characteristics of coronary vessels are very different from those of pulmonary vessels, the multiscale filters and the decision criteria at different steps have to be redesigned for this application. In addition, the methods for the normalization of the multiscale response functions and the integration of the segmented vessels at multiple scales have to be designed to suit the coronary artery trees. Since
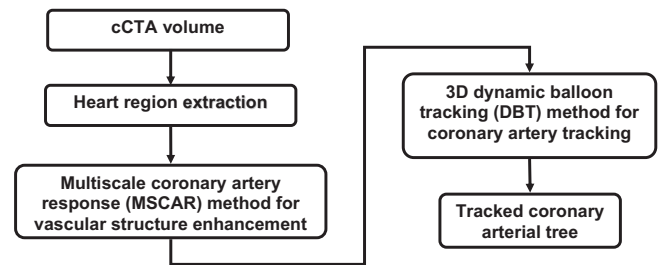

Fig. 1. Schematic diagram of our prototype coronary artery extraction algorithm using multiscale coronary artery response (MSCAR) segmentation and 3D dynamic balloon tracking (DBT), referred to as the MSCAR-DBT method.

the commercial vessel segmentation software is proprietary it is not possible to take advantage of the software already developed for this step. Furthermore, the digital files of the extracted coronary arteries by the clinical workstations are not accessible to the user so that we cannot utilize the extracted coronary arteries as input to our plaque detection system. We plan to use the original cCTA scan as input to our CADe system and the coronary artery extraction process will be a built-in preprocessing step. In this pilot study, we evaluated our prototype method for segmentation and tracking of the coronary arterial tree in a small data set and compared the performance of our method with a clinically used commercial workstation that segments and displays coronary arterial trees for radiologist's visualization.

2. Materials and methods

2.1. Materials

A data set containing 20 ECG-gated contrast-enhanced cardiac CTA scans was used for the performance comparison in this study. The CTA scans were retrospectively collected from patient files at the University of Michigan Hospital with Institutional Review Boards (IRB) approval. The CTA scans were acquired with GE multidetector CT scanners, 120–140 kVp, 300–600 mAs, reconstructed at 0.625 mm slice thickness. A single reconstructed phase (70% or 75%) was selected for each scan. Calcified plaques, non-calcified soft plaques and mixture of calcified and non-calcified soft plaques were found in 19 of the 20 cases and the remaining case was determined to be normal during clinical diagnosis.

2.2. MSCAR-DBT: coronary artery extraction method

Fig. 1 shows the schematic diagram of our prototype automated segmentation and tracking method for the coronary arteries. The method includes three major steps: heart region extraction, vascular structure enhancement and segmentation, and coronary artery tracking [26]. The air region outside the patient body was first excluded by thresholding at a voxel value of 50. To extract the heart region, the EM segmentation method [27] was applied to the body region in the volume of the cCTA scan assuming there were two classes of structures in the volume: lung region containing the air as class 1 and the other structures not belonging to class 1 as class 2. After EM segmentation, the structures of chest wall, the pulmonary vascular structures and heart region were segmented as class 2. To separate the heart region from the chest wall and to remove the pulmonary vascular structures, a morphological erosion operation was applied to class 2. It was experimentally found that a spherical structuring element with 25 mm in diameter was large enough to shrink the heart and chest wall, but would not eliminate the heart region because the hearts were larger than the spherical structuring element. Therefore the morphological erosion could separate the connection of the heart with the chest wall. The heart region was
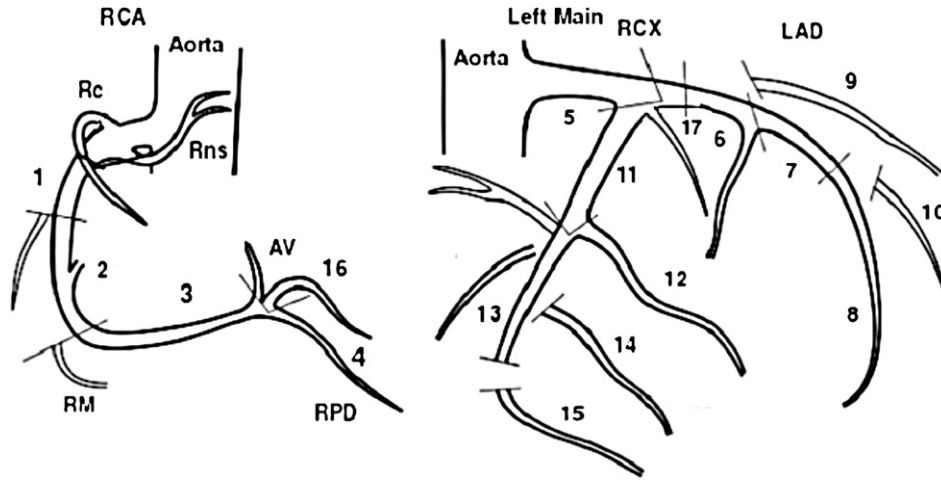
Fig. 2. Seventeen major coronary arterial segments [28] that are considered clinically significant. (1) Proximal RCA, (2) mid RCA, (3) distal RCA, (4) right posterior descending (RPD) artery, (5) main LCA, (6) Proximal left anterior descending (LAD), (7) Mid LAD, (8) apical LAD, (9) first diagonal, (10) second diagonal, (11) proximal left circumflex (LCx) artery, (12) first obtuse marginal (OM1), (13) distal, LCx, (14) second obtuse marginal (OM2), (15) posterior descending (PD), (16) posterior lateral branch (PLB), and (17) ramus intermedius segment.

finally extracted by applying a morphological dilation operation to the largest region which was separated by the erosion operation using the same structuring element.

We have designed a vessel segmentation method, referred to as the multiscale coronary artery response (MSCAR) method, for coronary artery segmentation. To adaptively segment the coronary vessels, the VOI enclosing the heart is first convolved with the second derivatives of 3D Gaussian functions with different variances (multiple scales) to cover the coronary arteries of a range of diameters. The eigenvalues of the 3D Hessian matrix are calculated at each voxel of the filtered volume at each scale. The eigenvalues for the voxels contain important shape information such that the eigenvalues corresponding to a linear structure will be different from those corresponding to a nonlinear structure, noise, or no structure. To enhance a structure of interest, a response function that combines the eigenvalues should be designed properly to maximize the response for the given structure. For example, a response function for a line structure such as a vessel is different from that for a blob-like object such as a nodule. The response of the enhancement filter also depends on the scale of the filter. It reaches a maximum when the scale of the filter matches the size of the structure. A vascular tree contains at least two major types of structures: the vessels that can be described as line structures and the bifurcations that can be described as blob-like structures. Conventional response functions [15,20,23] do not work well for vascular trees. For example, a line response function will suppress the bifurcations and leave gaps at the bifurcation points, cutting off the branch from the main vessel. We have designed a new multiscale response function [25] using the eigenvalues of the Hessian matrix that can enhance vascular structures including bifurcations and to suppress non-vessel structures. The response function is briefly described below.

For a voxel at $\bar{r} = (x, y, z)$, let the eigenvalues of the Hessian matrix be $\lambda_1(r)$, $\lambda_2(r)$ and $\lambda_3(r)$, where $\left| \lambda_1(r) \right| > \left| \lambda_2(r) \right| > \left| \lambda_3(r) \right|$, and their corresponding eigenvectors be $e_1(r)$, $e_2(r)$ and $e_3(r)$. The eigenvector $e_i(r)$ represents the direction along which the second derivative represented by $\lambda_i(r)$, $i = 1, 2, 3$, is maximum. The three eigenvalues have intuitive characteristics in discriminating structures of different shapes. For example, for an ideal tubular structure in 3D volume, the eigenvalue $\lambda_3(r)$ will be approximately zero and the $\lambda_1(r)$ and $\lambda_2(r)$ will be approximately equal with larger magnitudes for the voxels at the centerline of the tube. Similarly, for an ideal sphere, the three eigenvalues will be equal at the center of the sphere. To utilize these characteristics, we have designed a multiscale response function R that has the following form [25] to enhance vascular structures including vessel bifurcations and suppress non-vessel structures:

$$R = \begin{cases} \dfrac{(|\lambda_1| + |\lambda_2|)}{2} \exp\left(- \left| \dfrac{|\lambda_1|}{\sqrt{\lambda_1^2 + \lambda_2^2 + \lambda_3^2}} - c \right| \right), & \lambda_1, \lambda_2, \lambda_3 < 0 \\ 0, & \text{otherwise} \end{cases} \tag{1}$$
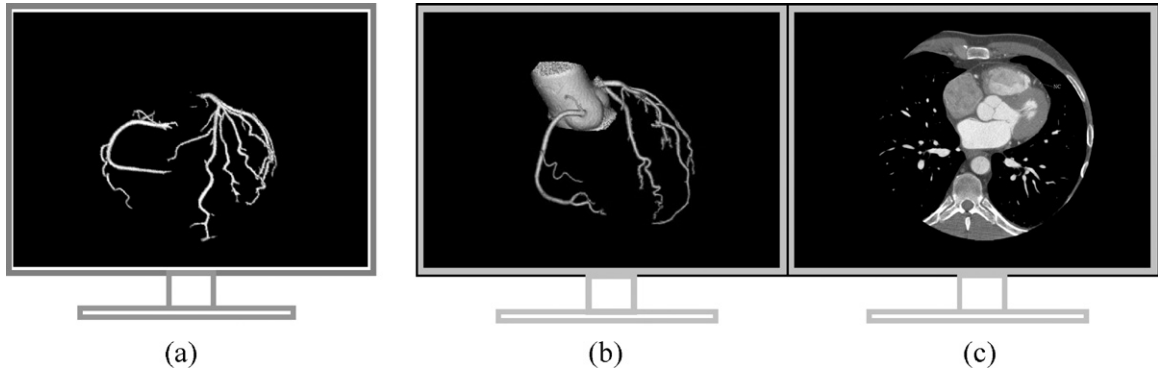

Fig. 3. The setting of visual assessment of automated segmentation and tracking of coronary arteries. (a) The PC with GUI displays the tracked coronary arteries rendered in 3D volume by our MSCAR-DBT method. (b), (c) the GE workstation displays the volume rendering of the coronary arteries obtained by the GE coronary analysis software, and the original cCTA scan.
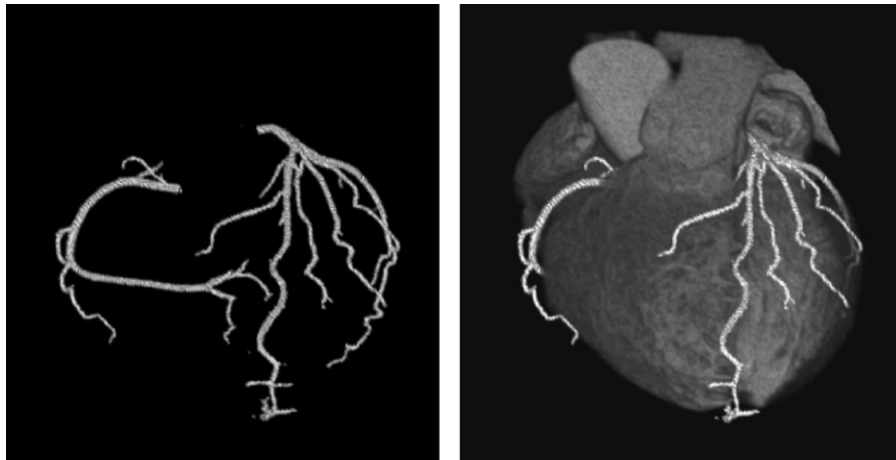
Fig. 4. An example of coronary arterial trees extracted by our MSCAR-DBT method. Left: the computer tracked coronary arteries rendered in 3D volume. Right: the computer tracked coronary arteries superimposed on the heart.

where the value of the constant c determines the strength of the response for each types of structures. The significance of c in the response function was discussed in our previous study [25]. For enhancement of both tubular structures and vessel bifurcations, the value of c was estimated to be 0.7.

In this preliminary study, we evaluated 3D Gaussian filters at four scales corresponding to vessel sizes ranging from 1 mm to 8 mm in diameter. At each scale, the response function value at each voxel is calculated from the eigenvalues using Eq. (1) over a

VOI containing the entire heart region. In this enhanced VOI, two classes of voxels are assumed [1] the voxels with a high response indicate that there is an enhanced vessel and its size matches the given filter scale, and [2] the voxels with a low response value that might contain structures to be suppressed such as a structure that does not match the filter size. The EM estimation is then applied to the VOI to segment the vessels by extracting the high response voxels at this single scale. The voxels in the low response class are set to a background value of 0 after EM segmentation. To normalize the
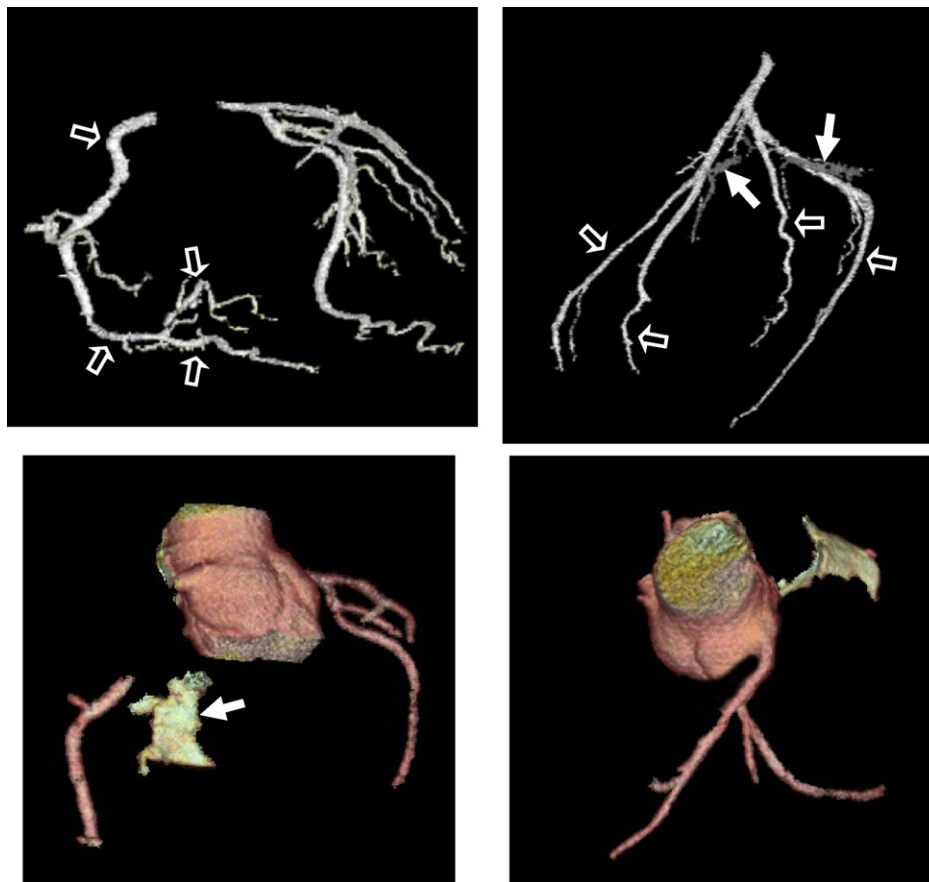

Fig. 5. An example of the left and right coronary artery trees extracted by our MSCAR-DBT method (top row) and GE software (bottom row). The open white arrows point to four FNs in LCA and four FNs in RCA by GE method. The white arrows point to one FPs and two FPs by GE method and our MSCAR-DBT method, respectively. There is no FN by our method in this case.
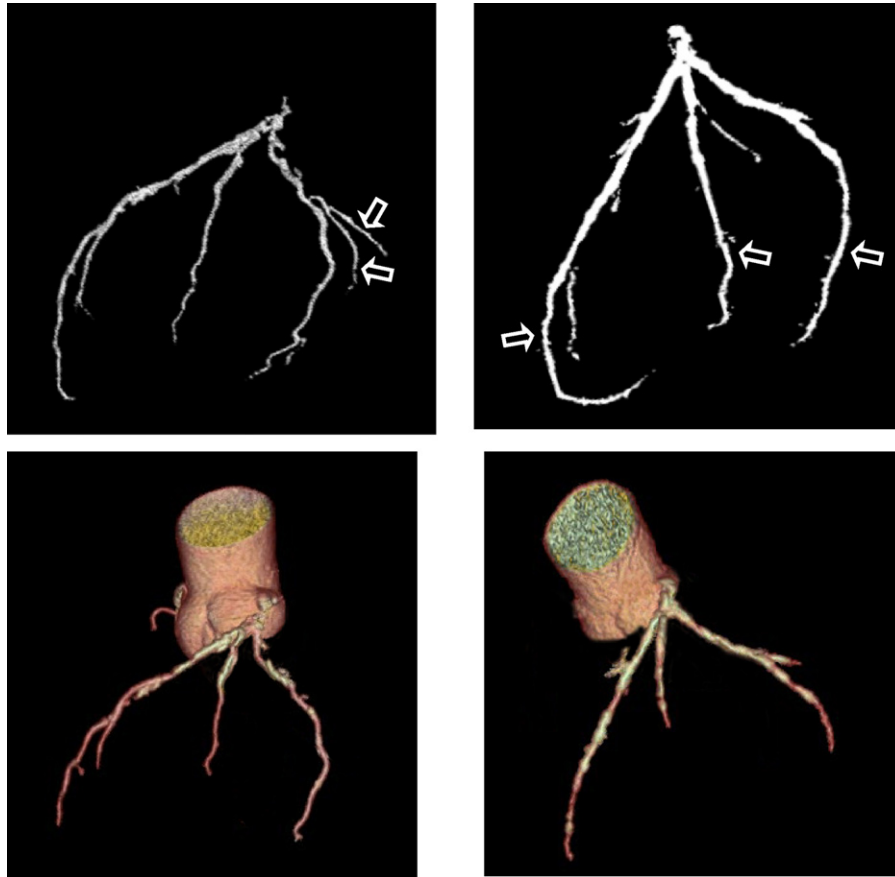
Fig. 6. Examples of left coronary artery trees extracted by our MSCAR-DBT method (top row) and GE software (bottom row) for two cases (left and right column). The open white arrows point to two FNs by the GE software but tracked by our MSCAR-DBT method for one case (left column) and three FNs by the GE software for another case (right column). There is no FN or FP by our MSCAR-DBT method and no FP by the GE software for both coronary trees.

response function value so that the responses are comparable for the different scales, the output of the convolution with the second derivative of the Gaussian filter at scale i is multiplied by a normalization factor σ_i^2, where σ_i^2 is the variance of the Gaussian filter. The extracted structures in the VOI at multiscales are combined into a single volume of extracted structures with voxel values $v(x, y, z)$ by applying the maximum operation to the corresponding voxels in all scales:

$$v(x, y, z) = \max\{R_i^n(x, y, z), i = 1, \ldots 4\} \tag{2}$$

where $R_i^n(x, y, z)$ is the normalized response at scale i and voxel location (x, y, z).

After MSCAR is applied to the heart region, not only the coronary arteries but also the coronary veins and other vessel-like noise structures are enhanced and segmented. To construct the coronary arterial trees, we have designed a 3D dynamic balloon tracking (DBT) method to track the coronary arteries. In this preliminary study, the tracking algorithm started at two manually identified seed points located at the origins of the left and right coronary artery (LCA and RCA), respectively, to track the left and right coronary arterial trees for each case. The tracking after the seed point identification is fully automated. A sphere is generated with the starting point as the center. The DBT algorithm searches for connected components intersecting the sphere surface and determines if an intersecting structure is a possible vessel by analyzing its characteristics. The criteria of moving the sphere to an intersecting structure includes [1] the intersecting structure is compact and approximately a round shape [2] the direction of the sphere moving to the center of the intersection is less than 90°, and [3] the size of the new sphere derived from the intersecting structure is smaller

than 1.5 times of the current sphere to avoid moving the sphere to a large noisy structure because the sphere is designed to move from the larger vessels to smaller vessels starting at the origin of the coronary arterial tree. If the above criteria are satisfied, the center of the intersection will be taken as the next tracking point. The sphere will be moved and centered at this new tracking point and the diameter of the sphere is adjusted to enclose the diameter of the vessel. As the tracking proceeds along the vessel, the diameter of the sphere is varied adaptively like a balloon according to the local vessel size. At each tracking point, a similar search process will be performed. The DBT algorithm searches for possible intersections between the balloon surface and vessel branches as well as the continuation of the current vessel. All the possible branches are labeled and stored in a queue. The DBT algorithm will start from the next branch in the queue after tracking of the current vessel ends. The tracking of each branch continues until the stopping criteria have been satisfied. The current criteria are set to be [1] the tracked vessel reaches a predetermined minimum vessel diameter, or [2] tracking has extended beyond the predetermined region, such as the boundaries of the heart volume. The above procedure is repeated until the queue is empty. The vessel tree is formed by following the trajectory of the dynamic balloon.

2.3. Performance evaluation

The coronary arterial trees of all 20 test cases were extracted by our MSCAR-DBT method as described above. The same data set was processed by the GE Advantage workstation (version 4.4, GE Healthcare, Wauwatosa, WI). The GE software can extract the coronary arterial trees automatically without user-identified seed
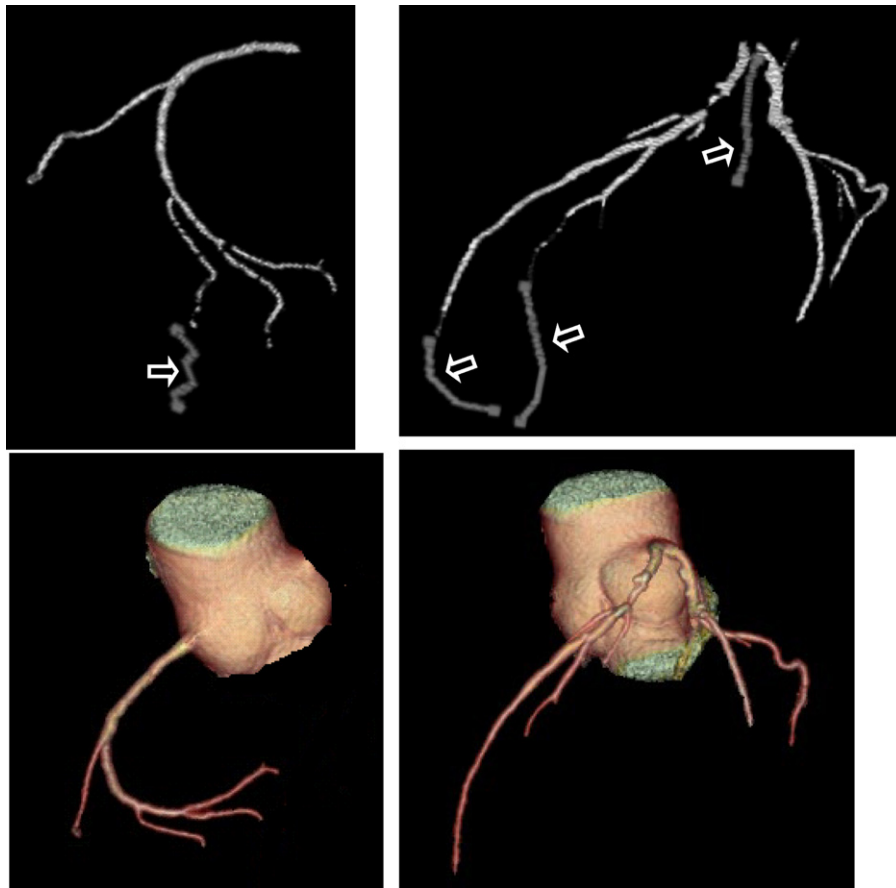
Fig. 7. An example of left and right coronary artery tree extracted by our MSCAR-DBT method (top row) and GE software (bottom row). The RCA and LCA are shown in left column and right column, respectively. One segment in RCA and 3 segments in LCA (pointed by open white arrows) were missed by both methods. These FN segments (darker vessels in top rows) were manually tracked by a radiologist to show the missing parts.

points. However, for the cases that the GE software failed to extract a coronary arterial tree due to the failure of starting point identification, seed points were manually input to the GE tracking software by clicking the mouse to start the vessel tracking. In our data set, the seed points were manually input for two out of the 40 coronary trees.

Because the digital files for the segmented vessels were not accessible on the commercial GE workstation, the coronary artery extraction performance of our method and the GE software were compared based on visual assessment of the segmented vessels by experienced cardiothoracic radiologists. Seventeen major coronary arterial segments [28] (Fig. 2) that are considered clinically significant were used as the reference for the visual assessment: (1) proximal RCA, (2) mid RCA, (3) distal RCA, (4) right posterior descending (RPD) artery, (5) main LCA, (6) Proximal left anterior descending (LAD), (7) Mid LAD, (8) apical LAD, (9) first diagonal, (10)
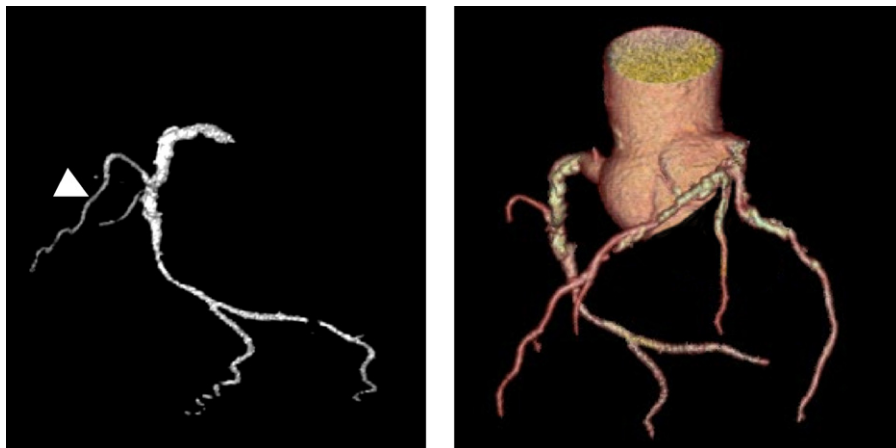

Fig. 8. An example of coronary artery tree extracted by MSCAR-DBT method (left) and GE software (right). A long arterial segment in RCA (white arrowhead) not tracked by the GE software, was not counted as an FN for the GE software nor as FP for our MSCAR-DBT method, because it is not one of the 17 coronary arterial segments that are considered clinically significant. The LCA of this case is also shown in left column of Fig. 6.

second diagonal, (11) proximal left circumflex (LCx) artery, (12) first obtuse marginal (OM1), (13) distal, LCx, (14) second obtuse marginal (OM2), (15) posterior descending (PD), (16) posterior lateral branch (PLB), and (17) ramus intermedius segment.

Volume rendering of the coronary vessel trees tracked by our method was displayed on a PC using an in-house developed graphical user interface (GUI). The PC was placed next to the GE workstation which displayed the original cCTA scan and the coronary vessel trees obtained by the GE coronary analysis software. Fig. 3 shows the setting of the PC and GE workstation. For each case, the radiologist visually examined the original coronary cCTA scan and compared the volume rendered coronary arteries to identify untracked segments (false negatives, FNs) and mistakenly tracked veins and noisy structures (false positives, FPs). Two experienced cardiothoracic radiologists assessed the 20 cases independently. For vessel segments that the two radiologists' readings did not agree, the case was re-read to obtain a consensus. The FN vessel segments and FPs agreed upon by both radiologists were used for the performance evaluation. The coronary arteries that were not on the list of the 17 coronary segments were not counted as FP or FN.

3. Results

Fig. 4 shows an example of coronary arterial tree extracted by our MSCAR-DBT method. Table 1 Table 1 shows the number of FN and FP segments by our MSCAR-DBT method and by the GE software identified by the two radiologists. For the visible coronary arterial segments in the 20 cases, the radiologists identified that 25 segments were missed by our MSCAR-DBT method, ranging from 0 to 5 FN segments in individual case, and that 55 artery segments were missed by the GE software, ranging from 0 to 7 FN segments

Table 1
The number of FN and FP segments by our multiscale coronary artery response-dynamic balloon tracking (MSCAR-DBT) method and by the GE advantage workstation software.

	False negatives			False positives		
	LCA	RCA	Total	LCA	RCA	Total
MSCAR-DBT method	17	8	25	13	6	19
GE workstation software	32	23	55	10	5	15

in individual cases. 19 and 15 FPs were identified in our and the GE coronary trees, respectively, ranging from 0 to 4 FPs for both methods in individual cases. The average and the standard deviation of FNs were 1.25 ± 1.68 segments/case and 2.75 ± 2.25 segments/case for MSCAR-DBT and GE software, respectively. The average and the standard deviation of FPs were 0.95 ± 1.32 segment/case and 0.75 ± 1.1 segment/case for MSCAR-DBT and GE software, respectively.

Wilcoxon signed rank test was used to test the significance of the difference in performance between our MSCAR-DBT method and the GE software. The test results show that the difference in the number of FN segments/tree was statistically significant for both LCA ($p < 0.02$) and RCA ($p < 0.05$), but the difference in the number of FP segments/tree did not achieve statistical significance for either LCA ($p > 0.49$) or RCA ($p > 0.96$).

Examples of coronary trees tracked by the MSCAR-DBT and the GE methods, and the scoring of the FPs and FNs by radiologists, are shown in Figs. 5, 6 and 7. Note that some of the vessels in the examples segmented by MSCAR-DBT appear discontinuous occasionally but these are artifacts from our display software. The vessels shown were connected because they were tracked by the DBT.
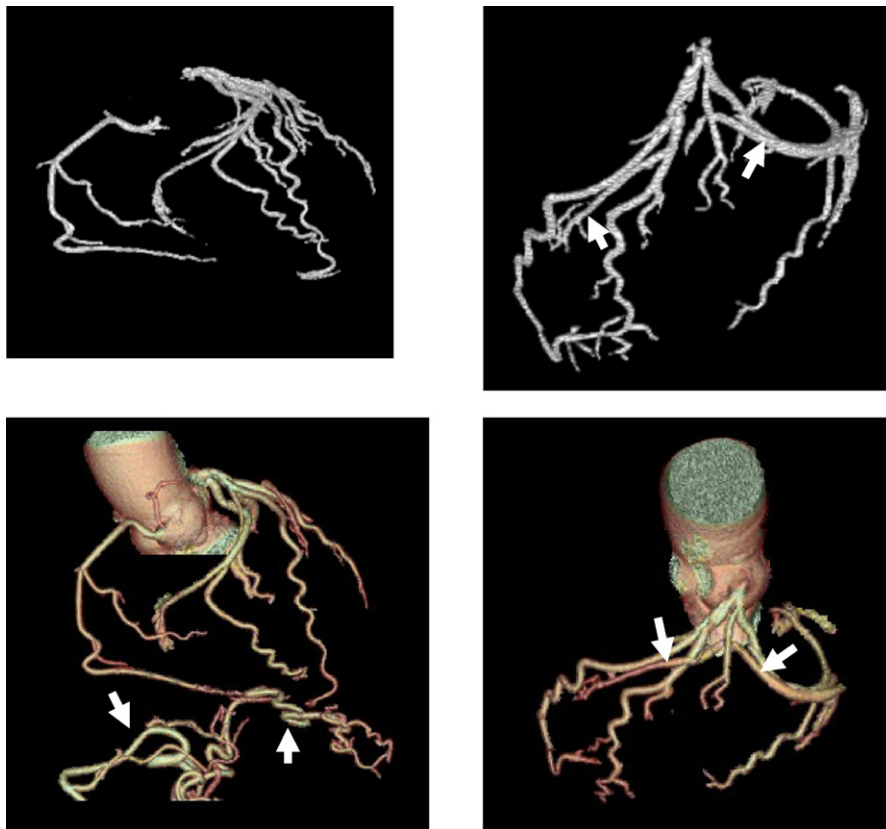

Fig. 9. An example of the counting of FPs for coronary artery tree extracted by our MSCAR-DBT method (top row) and the GE software (bottom row). A large connected component composing of abdominal vessels was visually separated into two FPs by radiologists, in term of their location, at the left and right side of the heart (white arrows). The two venous segments (white arrows in right column) were counted as two FPs for both methods.
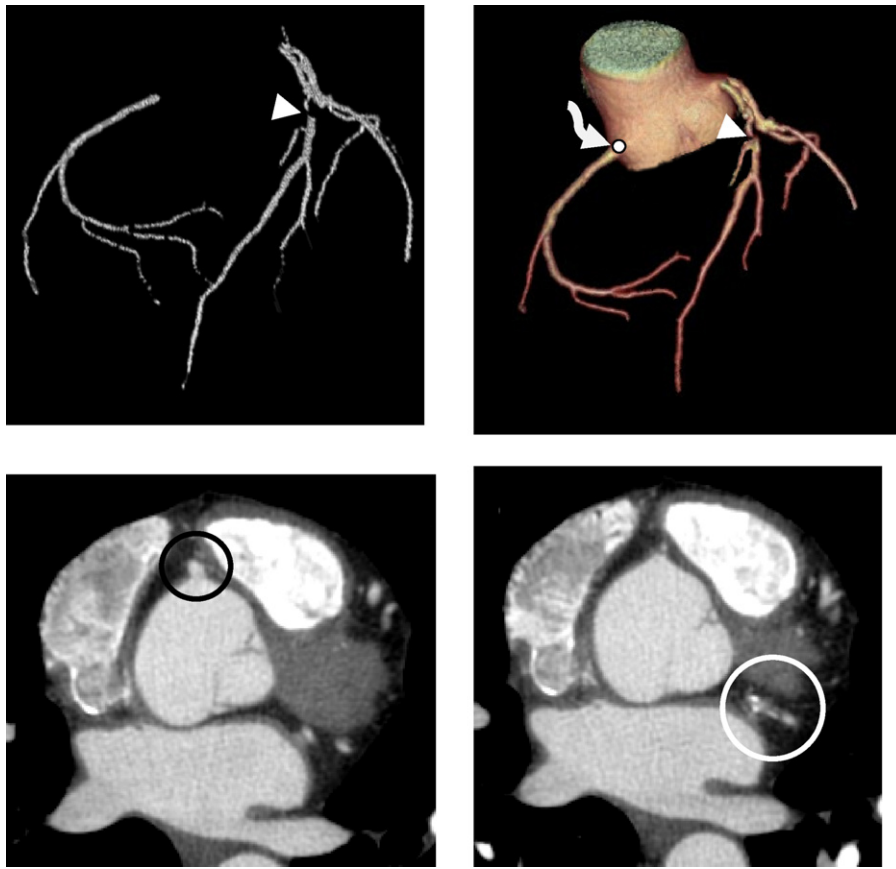
Fig. 10. An example shows a seed point (white dot pointed by white curved arrow in top right image) was manually input to RCA due to the failure of the GE software in identifying the seed point, the corresponding seed region (black circle) is shown in the original cCTA scan (bottom left). The calcified plaques (white circle in bottom right image) in the LAD caused a gap (white arrowhead) both in the coronary artery tree extracted by our MSCAR-DBT method (top left) and the GE software (top right).

4. Discussions

Quantitative evaluation of vessel segmentation accuracy and the completeness of vessel tree construction is challenging because there is no ground truth for the vessel tree for clinical cases. Although a tubular phantom can be constructed with known "vessels," it is difficult to construct a realistic phantom with a complete vessel tree mimicking complicated vascular structures and other anatomical structures that may cause errors during tracking. In our previous study [25] that an automated vessel segmentation method was developed for pulmonary vessel tree construction in CTPA images, two patient cases were chosen as representative cases from our collected data set as the test set for the performance evaluation of our vessel tree extraction method. Two experienced thoracic radiologists provided reference standard for the pulmonary vessels including arteries and veins by manually tracking the vessel tree and marking the center of the vessels using a graphical user interface. The accuracy of the vessel tree segmentation was evaluated by the percentage of the reference standard vessel center points overlapping with the segmented vessels. However, manual tracking and marking the center points of the vessels are very time consuming. Schaap et al. [29] developed a framework for the evaluation of coronary artery centerline extraction method. The framework encompasses a publicly available database containing 32 coronary CTA scans with corresponding reference standard centerlines derived from manual annotation by three trained observers. Only four vessels were selected for annotation for each cCTA scan. The first three vessels were always the RCA, LCA, and LCX. The fourth vessel was selected from the large side-branches of the above major

coronary arteries. Although the benefit of the public data set is clear for quantitative evaluation of coronary artery extraction, the above framework is limited to the evaluation of centerline extraction for the four chosen coronary arteries. Because the coronary artery tree contains more than four vessels, the completeness of the coronary artery tree cannot be evaluated using this public database. Plaques in an arterial segment will not be detected if the segment is missed in the vessel extraction process. Despite the intensive labor, it would be possible to select several representative cases and manually mark the vessel center points for a complete vessel tree using a similar performance evaluation protocol as that in our previous study [25]. However, this approach can only be used to evaluate our coronary artery tree extraction method but not the clinical software such as the GE software because the digital files of the extracted vessel tree by the clinical software are not accessible to the user. Currently, the best alternative would be the visual assessment by experienced cardiothoracic radiologists. To reduce the bias of subjective visual assessment, the agreement between two radiologists was used in our study.

In our study, the coronary arteries that were not one of the 17 reference segments were ignored and were not counted as FP or FN. Fig. 8 shows an example in which a long arterial segment in RCA was not segmented by the GE software, but it was not counted as an FN because it was not one of 17 coronary arterial segments. A limitation of visual assessment of the coronary artery tree extraction is the counting of FPs such as the noisy structures, the veins or other vessels that were mistakenly extracted as coronary arteries. Fig. 9 shows an example in which a large connected structures composed of a number of abdominal vessels
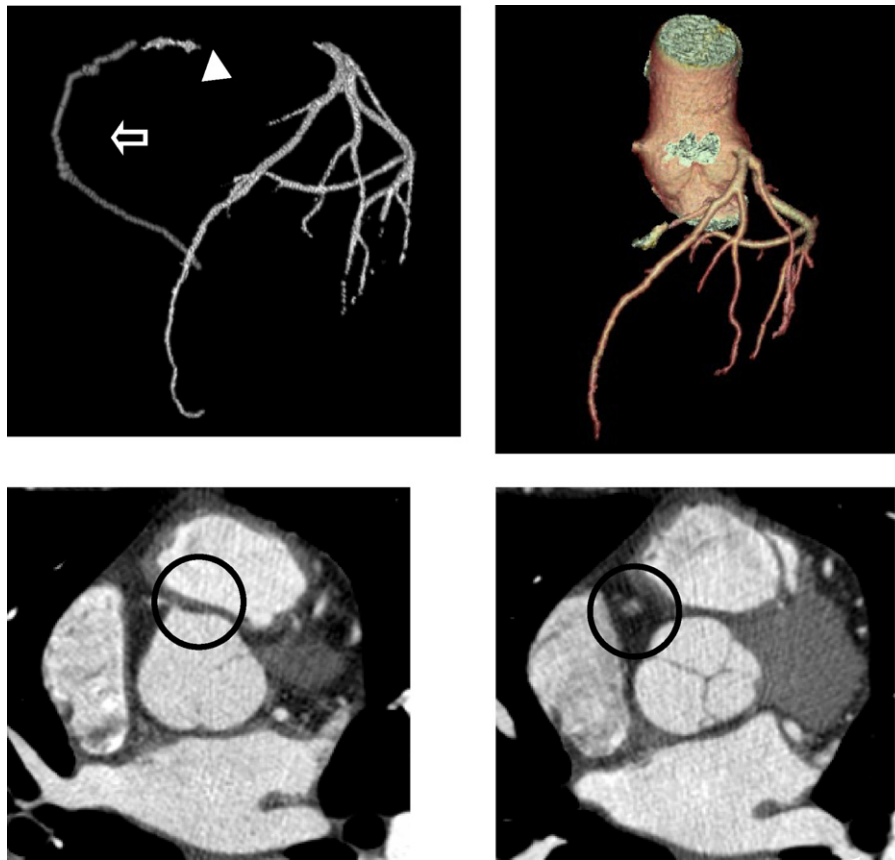
Fig. 11. An example of a failure in the tracking of the RCA due to the motion blur artifacts for both our MSCAR–DBT method (top left) and the GE software (top right). The FN segment (darker vessels pointed by open white arrow) was manually tracked by a radiologist to show the missing part. Two axial view images separated by 8 slices (bottom row) show the short starting vessel segment without motion (black circle, bottom left) that was extracted (white arrowhead) by our method, and the later segment with motion (black circle, bottom right) that failed to be tracked by either our method or the GE software.

were extracted by the GE software. It is difficult to define criteria to separate the connected vessels into individual vessel segments or branches. For this case, both radiologists agreed to separate the large connected vascular structure into two components according to their anatomic locations and count them as one FP on the right side and one FP on the left side of the heart. For the same case, two venous segments adjacent to the left coronary tree were also extracted by both methods, and were counted as two FPs without hesitation by both radiologists because they were separate segments.

In this preliminary study, our DBT method used two starting points manually identified at the origins of the left and right coronary tree as the seed points, respectively, to track the left and right coronary arterial trees for each case. Although the GE software can extract the coronary arterial trees automatically without user-identified seed points, the seed points were manually input for two out of the 40 coronary trees in our data set due to the failure of starting point identification by the GE software (Fig. 10). Most of the FNs were caused by artifacts of heart motion that blurred the coronary artery segments, and the low contrast filled arteries due to blockage by plaques. Fig. 10 shows an example that a gap was caused by the calcified plaques in the LAD segment for both our MSCAR–DBT method and the GE software. The DBT method can jump over a gap if the gap is small compared to the diameter of the local balloon. In this preliminary study, a single reconstructed phase (70% or 75%) was selected for each scan. The RCA generally has greater motion during late diastole of the cardiac circle (>65%), and the motion artifacts can cause failure in tracking the RCA. Fig. 11 shows an example of a failure in the tracking of the RCA due

to motion blur artifacts for both our MSCAR–DBT method and the GE software.

As shown in Table 1, the results of our preliminary study indicated that the performance of the MSCAR–DBT algorithm was superior to that of a commercial system in this small data set. However, the estimated performance may be biased optimistically because it was not evaluated on an independent test set, whereas it was for the commercial system. Nevertheless, the preliminary results are encouraging and further development of this technique is warranted. The use of an in-house developed coronary artery segmentation and tracking algorithm in the prescreening stage of our automated plaque detection system allows us the flexibility of optimizing all image processing stages as a whole. More importantly, the automated CADe system to be developed will be less dependent on specific commercial software and can be more easily adapted to coronary CTA scans acquired with CT scanners from different manufacturers.

5. Conclusion

The preliminary study demonstrates the feasibility that our MSCAR–DBT method can enhance and segment the vascular structures and track coronary artery trees. Although both our method and the GE software can extract coronary artery trees reasonably well and the performance of our method is superior to that of GE software in a small data set, both methods are far from perfect in extracting coronary artery trees automatically, especially for the artery segments affected by motion artifacts, severe calcified and

non-calcified soft plaques, and the false tracking of the veins and other noisy structures. Fully automated and accurate extraction of the coronary arteries is a very important task for our in-house development of a CADe system for plaque detection, and for a commercial system to provide radiologists an efficient visualization tool for vessel analysis in clinical practice. Further studies are underway to develop methods for identification of seed points automatically and for improvement of the segmentation and tracking accuracy, and ultimately develop computer-vision methods to automatically detect soft plaques along the tracked arteries.

Acknowledgments

References

[1] Budoff MJ, Achenbach S, Blumenthal RS, Carr JJ, Goldin JG, Greenland P, et al. Assessment of coronary artery disease by cardiac computed tomography: a scientific statement from the american heart association committee on cardiovascular imaging and intervention, council on cardiovascular radiology and intervention, and committee on cardiac imaging, council on clinical cardiology. Circulation 2006;114:1761–91.

[2] Writing Group MembersLloyd-Jones D, Adams R, Carnethon M, De Simone G, Ferguson TB, et al. Heart disease and stroke statistics—2009 update: a report from the American Heart Association Statistics Committee and Stroke Statistics Subcommittee. Circulation 2009;119:e21–181.

[3] Fine JJ, Hopkins CB, Ruff N, Newton FC. Comparison of accuracy of 64-slice cardiovascular computed tomography with coronary angiography in patients with suspected coronary artery disease. Am J Cardiol 2006;97:173–4.

[4] Budoff M, Dowe D, Jollis J, Gitter M, Sutherland J, Halamert E, et al. Diagnostic performance of 64-multidetector row coronary computed tomographic angiography for evaluation of coronary artery stenosis in individuals without known coronary artery disease: results from the prospective multicenter ACCURACY (Assessment by Coronary Computed Tomographic Angiography of Individuals Undergoing Invasive Coronary Angiography) trial. J Am Coll Cardiol 2008;52:1724–32.

[5] Min J, Shaw L, Devereux R, Okin P, Weinsaft J, Russo D, et al. Prognostic value of multidetector coronary computed tomographic angiography for prediction of all-cause mortality. J Am Coll Cardiol 2007;50:1161–70.

[6] Garcia M, Lessick J, Hoffmann M, Investigators CS. Accuracy of 16-row multidetector computed tomography for the assessment of coronary artery stenosis. JAMA 2006;296:403–11.

[7] Masutani Y, Macmahon H, Doi K. Automated segmentation and visualization of the pulmonary vascular tree in spiral CT angiography: an anatomy-oriented approach based on tree-dimensional image analysis. J Comput Assist Tomogr 2001;25:587–97.

[8] Rubin GD, Paik DS, Johnston PC, Napel S. Measurements of the aorta and its branches with helical CT. Radiology 1998;206:823–9.

[9] Higgins WE, Spyra WJT, Warwoski RA, Ritman EL. System for analyzing high-resolution three dimensional coronary angiograms. IEEE Trans Med Imaging 1996;15:377–85.

[10] Blanks RG, Wallis MG, Given-Wilson RM. Observer variability in cancer detection during routine repeat (incident) mammographic screening in a study of two versus one view mammography. J Med Screen 1999;6:152–8.

[11] Chung A, Noble J. Statistical 3D vessel segmentation using a Rician distribution. Int Conf Med Image Comput Comput-assist Interv 1999;1679:82–9.

[12] Kutka R, Stier S. Extraction of line properties based on direction fields. IEEE Trans Med Imaging 1996;15:51–8.

[13] McInerney T, Terzopoulos D. T-snake: topology adaptive snakes. Med Image Anal 2000;4:73–91.

[14] Lorigo LM, Faugeras OD, Grimson WEL, Keriven R, Kikinis R, Nabavi A, et al. Curves: curve evolution for vessel segmentation. Med Image Anal 2001;5:195–206.

[15] Krissian K, Malandain G, Ayache N, Vaillant R, Trousset Y. Model-based detection of tubular structures in 3D images. Comput Vision Image Understanding 2000;80:130–71.

[16] Kanazawa K, Kawata Y, Niki N, Satoh H, Ohmatsu H, Kakinuma R, et al. Computer-aided diagnosis for pulmonary nodules based on helical CT images. Comput Med Imaging Graph 1998;22:157–67.

[17] Frangi AF, Neissen W, Vincken K, Viergever M. Multiscale vessel enhancement filtering. Med Image Comput Comput-Assist Interv 1998;1496:130–7.

[18] Lorenz C, Carlsen I, Buzug T, Fassnacht C, Weese J. A multi-scale line filter with automatic scale selection based on the Hessian matrix for medical image segmentation. In: Proceedings of the First International Conference on Scale-Space Theory in Computer Vision. 1997. p. 152–63.

[19] Aylward S, Bullitt E. Initialization, noise, singularities, and scale in height ridge traversal for tubular object centerline extraction. IEEE Trans Med Imaging 2002;21:61–75.

[20] Li Q, Sone S, Doi K. Selective enhancement filters for nodules, vessels, and airway walls in two- and three-dimensional CT scans. Med Phys 2003;30:2040–51.

[21] Shikata H, Hoffman EA, Sonka M. Automated segmentation of pulmonary vascular tree from 3D CT images. Proc SPIE Med Imaging 2004;2004:107–16.

[22] Bülow T, Lorenz C, Renisch S. A general framework for tree segmentation and reconstruction from medical volume data. Med Image Comput Comput-Assist Interv 2004.

[23] Sato Y, Nakajima S, Shiraga N, Atsumi H, Yoshida S, Koller T, et al. Three-dimensional multi-scale line filter for segmentation and visualization of curvilinear structures in medical images. Med Image Anal 1998;2:143–69.

[24] Metz CT, Schaap M, Weustink AC, Mollet NR, van Walsum T, Niessen WJ. Coronary centerline extraction from CT coronary angiography images using a minimum cost path approach. Med Phys 2009;36:5568–79.

[25] Zhou C, Chan HP, Sahiner B, Hadjiiski LM, Chughtai A, Patel S, et al. Automatic multiscale enhancement and hierarchical segmentation of pulmonary vessels in CT pulmonary angiography (CTPA) images for CAD applications. Med Phys 2007;34:4567–77.

[26] Zhou C, Chan HP, Chughtai A, Patel S, Agarwal P, Hadjiiski LM, et al. Automated segmentation and tracking of coronary arteries in ECG-gated cardiac CT scans. Proc SPIE 2008;6915:001–7.

[27] Dempster NM, Laird AP, Rubin DB. Maximum likelihood from incomplete data via the EM algorithm. J R Statist Soc B 1977;39:185–97.

[28] Austen WG, Edwards JE, Frye RL, Gensini GG, Gott VL, Griffith LS, et al. A reporting system on patients evaluated for coronary artery disease. Report of the Ad Hoc committee for grading of coronary artery disease, council on cardiovascular surgery, american heart association. Circulation 1975;51:5–40.

[29] Schaap M, Metz CT, van Walsum T, van der Giessen AG, Weustink AC, Mollet NR, et al. Standardized evaluation methodology and reference database for evaluating coronary artery centerline extraction algorithms. Med Image Anal 2009;13:701–14.